Deposition of Transparent Conducting Al-doped ZnO Thin Films by ICP-Assisted Sputtering

Ryota Shindo, Tadashi Iwata, Akinori Hirashima, Masanori Shinohara
Graduate School of Science and Technology
Nagasaki University
Nagasaki, Japan

Yoshinobu Matsuda
Department of Electrical and Electronic Engineering
Nagasaki University
Nagasaki, Japan
ymat@nagasaki-u.ac.jp

Abstract— **Aluminum-doped zinc oxide (AZO) is one of the promising transparent conductive oxide materials, which is expected to be an alternative to tin-doped indium oxide (ITO) that for long has been widely used in industry. The authors have been engaged in the development of AZO deposition process using inductively-coupled plasma assisted sputtering in a couple of years. This paper reports the results showing effectiveness of inductively coupled plasma (ICP) assisted sputtering in AZO film deposition process.**

Keywords-Zinc oxide; Transparent conducting oxide films; Sputtering ; Inductively-coupled plasma; Optical spectroscopy

I. INTRODUCTION

Transparent conducting oxide (TCO) films have been widely used as transparent conducting electrodes of various optoelectronic devices such as solar cells, flat panel displays, etc. Some TCO materials such as tin oxide and indium oxide have already been put to practical use in industry. In particular, tin-doped Indium oxide (ITO) has been mainly used so far due to its high transmittance in the visible region, high chemical stability and low resistivity. For the last ten years, however, aluminum-doped zinc oxide (AZO) received attention as one of the alternatives to the ITO. Though the AZO has lower inherent electric conductivity than ITO, it has advantages over ITO in environment resistance and resource cost. To actually replace ITO with AZO, however, a reproducible and highly-reliable fabrication process of good quality AZO thin films has to be developed. Thus, we have been investigating AZO film deposition process by using inductively coupled plasma (ICP) assisted sputtering.[1-6]

The advantages of ICP-assisted sputtering are as follows: 1) the target is sputtered with low target voltage and high target current, 2) the usage efficiency of the target is much improved due to the expansion of erosion area, 3) ionization and excitation of the sputtered particles are enhanced in the ICP and the enhanced ion fluxes to the substrate promote the crystallinity of thin films without intentional substrate heating, 4) lateral homogeneity of the deposited film is much improved.

Over the past several years, we have been investigating the ICP-assisted sputter-deposition process of AZO films by using the combination of a conventional planar magnetron and ICP [7], and we have recently verified the effectiveness of ICP-assisted sputtering by investigating particularly the ICP RF dependence of the discharge characteristic and the film properties.

This paper reports the experimental results of the discharge characteristic, measurements of metal atom densities, and the characteristic of thin film (deposition rate, resistivity, transmission, surface analysis) in the ICP assisted sputter-deposition process.

II. EXPERIMENT

Figure 1 shows the experimental setup for the ICP sputter-deposition of Al doped ZnO thin films.[8] A 3 inch DC planar magnetron, an argon gas supply system, a pumping system (turbo molecular pump and rotary pump combination), and a heater for baking were attached to the vacuum chamber (300nm in diameter and 300nm in height). After evacuating the chamber at an ultimate pressure of 3×10^{-6}Torr, argon gas was introduced at a flow rate of 50sccm by a mass flow controller. Then, the working pressure was set at 30mTorr by tuning the conductance of the main valve. A disk target of ZnO: Al_2O_3 (2wt%) of 60 mm diameter and 6mm thick was used as a target, and a glass substrate was set on an earthed substrate holder with a gap length of 80mm. Between the target and substrate, a single turn coil antenna of 100 mm diameter was installed and used for producing 13.56MHz inductively coupled plasma. The antenna was covered with insulator and water-cooled. The distance from the target to the RF coil and the distance from the RF coil to the substrate were both 40 mm. The magnetron plasma was generated by applying negative DC voltage to the target electrode, and the ICP was generated by applying 13.56MHz RF power to the coil antenna.

After thin film deposition, the substrate was taken out from the vacuum chamber and divided into several pieces of 10mm width each. Then the characteristic of each thin film (film thickness, resistivity, transmission, crystallinity, and elemental ratio) and their lateral distribution on the substrate were evaluated. The film thickness was measured by the stylus-profile meter (Mitsutoyo, SV-400). The electric conductivity was measured by four probe method, in which the film resistivity is evaluated by means of multiplying the experimental surface resistance by a geometrical correction factor determined by the film thickness, substrate geometry, and distance between probes. The optical transmission was measured by a spectral photometer consisting of a halogen lamp and an optical fiber-spectrometer (Ocean Optics, HR4000CG). In this work, we evaluated the optical transmittance of AZO films by using “the overall transmittance” that was averaged over visible wavelength range (380-780nm) and further averaged over lateral spatial distribution. An accurate optical characteristic, however, could

not be still evaluated by the overall transmittance mentioned above for films with different thickness. Thus, we evaluated an absorption coefficient α (absorbance per unit thickness) by $\alpha = \ln(1/T)/d$, where T is the transmittance, d is the film thickness. For example, let d =300nm and T = 90%; then this gives $\alpha = 0.4\ \mu m^{-1}$. The crystallinity of thin films was investigated by X-ray diffraction (RINGAKU, RINT2000). The elemental ratio in the film was measured by X-ray photoemission spectroscopy (SHIMADZU-KRATOS, AXIS-HS).

The behavior of sputtered particles in the gas phase was investigated by using the optical emission spectroscopy and the absorption spectroscopy. The optical emission spectra from the excited species were measured by an optical fiber spectrometer (Ocean Optics, HR4000CG-UV-NIR). Hollow cathode lamp (HDCL) absorption spectroscopy [9] was applied for the density measurement of ground-state metal atoms. The optical emission from a HCDL (Hamamatsu Photonics, L233-30NQ (Zn) or L233-13NB (Al)) was guided to a monochromator (JASCO, CT25) through the ICP-assisted sputtering chamber by lens, prism and optical fiber optics. The time modulated output signal from the photomultiplier tube (PMT) was monitored and averaged over 1024 times on a digital oscilloscope. By comparing the difference in the modulated amplitude of PMT output between plasma ON and OFF phases, absorbance was measured. The absorption measurements were done for Zn with 307.6 nm ($4s^2\ ^1S_0$-$4s5p\ ^3P_1^o$) and for Al with 396.15nm ($3s^23p\ ^2P_{3/2}^o$-$3s^24s\ ^2S_{1/2}$). It is noted here that the Zn 307.6 nm line is forbidden line. The use of absorption at the resonant line of Zn was impossible in this experiment due to too strong absorption. The sputtered atom density was obtained by comparing the experimental absorbance and the theoretical absorbance that was calculated by using an assumed gas temperature (400K) in both the light source and the target plasma, and by using assumed optical path length of 0.3m.

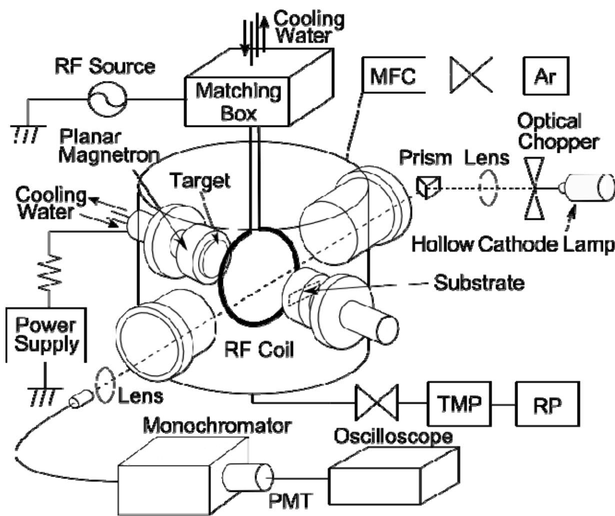

Figure1. Experimental Setup for the ICP sputter-deposition of Al doped ZnO thin films and for the absorption measurements of sputtered atoms.

III. Results and Discussion

The influence of ICP RF power on the discharge characteristic and thin film characteristic was investigated. In the following experiments, argon gas pressure was kept constant at 30mTorr, and the target discharge power (= input power to the planar magnetron) and ICP RF power (= input power to the ICP coil) were varied 0-50W and 0-300W, respectively.

A. ICP RF power dependence of discharge voltage and discharge current

Figure2 shows the ICP RF power dependence of the target discharge voltage and the target discharge current for the constant target input power at 45W. The target discharge voltage decreases and the discharge current increases with increasing ICP RF power. In other words, the impedance for the sputtering discharge decreases with the increase in ICP RF power. This is because the plasma density near the planar magnetron target is increased by the presence of ICP, whose density almost increases linearly with the ICP RF power. The decrease in the target discharge impedance under the ICP assisted sputtering is extremely effective because the low voltage sputtering is directly connected to the reduction of film damage on the substrate. Moreover, the low voltage sputtering is very effective for suppressing arcing. In addition, ICP assisted sputtering is effective for the improvement in the usage efficiency of the target and the uniformity of thin film characteristics because the sputtering area expands to the whole target surface.

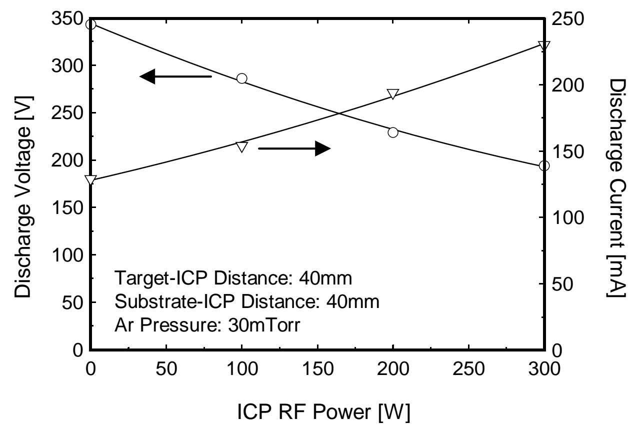

Figure2. ICP RF power dependence of discharge voltage (circle) and discharge current (triangle) during ICP assist magnetron sputtering at the working pressure of 30mTorr and at a constant target power of 45W.

B. ICP RF power dependence of optical emission spectra

The change in the plasma emission intensity by the presence or not of the ICP assist was investigated. The result is shown in Figure 3. From Figure 3(a), it is found that predominant optical emission lines are only due to the electron impact excitation of sputtered Zn atoms within the wavelength range from 200 to 400 nm without ICP assist. On the other hand, in the case of ICP assisted magnetron discharges, as shown in Figure 3(b), optical emission intensities for the Zn I lines are much increased, and additional optical emission lines from much higher excited states of Zn atoms and from excited

states of Al atoms are identified. The difference in the emission spectra between Figure 3 (a) and (b) is caused by the presence of additional excitation. Thus, the use of ICP assisted sputter-deposition having promoted excitation and ionization is effective for enhancing the crystallinity of deposited AZO films.

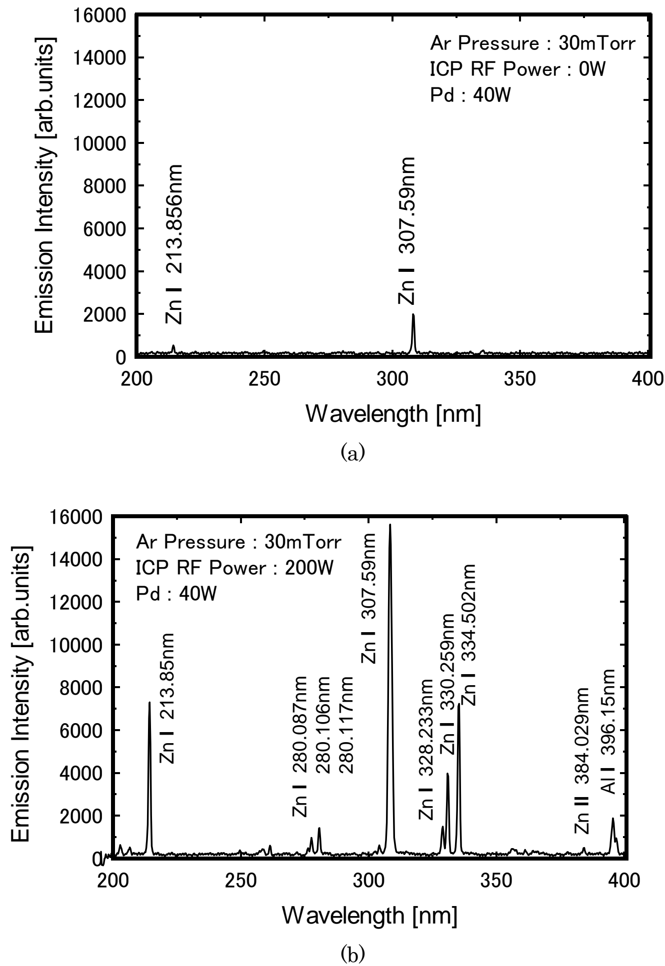

Figure3. Optical emission spectra for planar magnetron of 40W with ICP RF power of (a) 0W and (b) 200W.

C. ICP RF power dependence of metal atom densities

As we have described in the experimental section, number densities of sputtered atoms (Al and Zn) were measured by HDCL absorption spectroscopy. Figure 4 shows the experimental result for ICP RF power dependence of metal atom densities in gas phase. Both Zn and Al atom densities increases with increasing ICP RF power, but there is a difference in the tendency of ICP RF power dependence between Zn and Al atom densities. Al atom density monotonously increases with increasing ICP RF power, while Zn atom density increases 4 times with increasing ICP RF power from 0 to 100W, then saturates for ICP RF power more than 100 W. As for the absolute number density, it is noted that the Zn density is larger than Al density by 4 orders of magnitude. The atomic density ratio between Zn and Al is different from the element ratio in the AZO target. We are confident about the measurement of Al density, but we are not certain if the absolute value of Zn density is correct because we have used a forbidden line for the Zn absorption and the cross check has not completely done yet for Zn density. Thus, we would like to mention a qualitative comparison of both atom densities is worthwhile here. Thus, we notice the relative ratio of Al to Zn density increases with the increase in ICP RF power for the ICP RF power of more than 100 W. The difference in the ICP RF power dependence between Al and Zn atom densities is possibly predominantly caused by the large difference in both the standard enthalpy of formation (Al_2O_3: -1675.7 kJ/mol, ZnO: -348.0 kJ/mol) [10] and the ionization energy (Al: 5.99eV, Zn: 9.39eV). A more detailed analysis of the data in Fig. 4 is necessary.

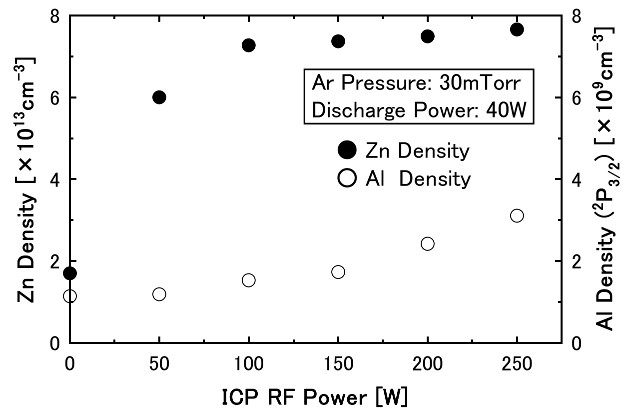

Figure4. ICP RF power dependence of Al and Zn atom densities during ICP assist magnetron sputtering at the working pressure of 30mTorr.

D. ICP RF power dependence of deposition rate

Figure 5 shows ICP RF power dependence of the spatial distribution of the deposition rate. It is found that the deposition rate increases by at most 20-30% with increasing ICP RF power from 0 to 300 W. Since the degree of the increase in deposition rate with increasing ICP RF power is smaller than that of atom densities shown in Figure 4, we can consider that a re-evaporation from the substrate probably occurred during the deposition process.

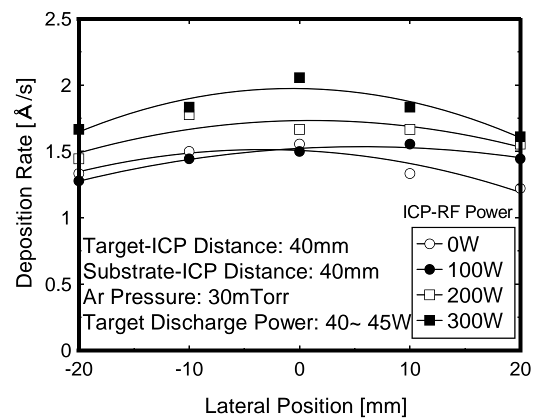

Figure5. ICP RF power dependence of deposition rate of AZO thin films.

E. ICP RF power dependence of resistivity

Figure 6 shows ICP RF power dependence of the spatial distribution of resistivity. The resistivity is very high about $2\times10^{-1}\Omega$cm for the planar magnetron discharge without ICP. However, the resistivity is drastically decreased and the uniformity is also improved with increasing ICP RF power. It is well known that for DC magnetron sputtering operating at a few mTorr the resistivity of the film is comparatively low both at the center and at very far radial positions from the center, while the resistivity is high at the substrate position just facing the target erosion area. On the other hand, in the present ICP assisted sputtering with operating pressure of 30mTorr, the spatial profile of resistivity is more uniform. The drastic decrease in the resistivity due to the ICP assist is explained as follows. When ICP RF power increases, the film damage decreases because the target voltage decreases, and the incident energy of particles to the substrate decreases. In addition to this effect, the total ion flux to the substrate with moderate energies of several electron volts increases due to the increase in plasma density with increasing ICP RF power. Thus, the crystallinity of films is improved by this moderate annealing effect to the substrate. It should be noted that highly conductive AZO films with resistivity of $2\times10^{-3}\Omega$cm are obtained with good uniformity by ICP assisted sputter-deposition.

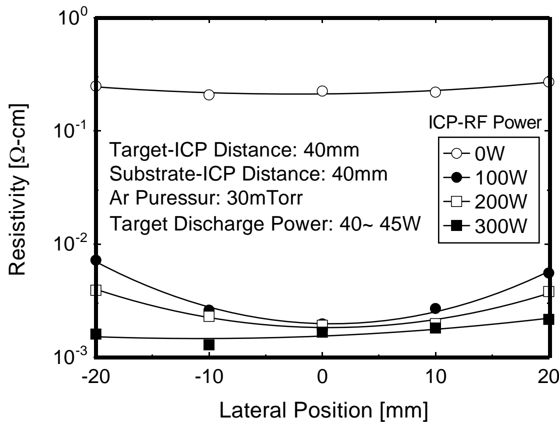

Figure6. ICP RF power dependence of resistivity of AZO thin films.

F. ICP RF power dependence of optical transmittance

Assisting ICP RF power is effective for increasing film transparency. Figure 7 shows ICP RF power dependence of the absorption coefficient of deposited AZO films. The vertical axis of Fig. 7 is the averaged absorption coefficient as explained in the experimental procedure. We judge the films with absorption coefficients of less than $0.5\mu m^{-1}$ have excellent optical transparency. Though the transmittance of deposited films is already satisfactory, the optical transparency is much improved for ICP RF power more than 100W as is shown in Fig.7.

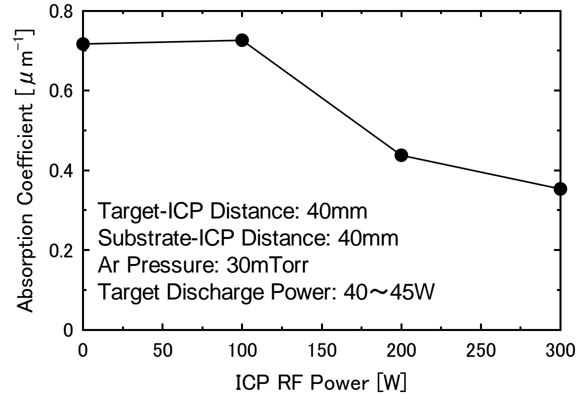

Figure7. ICP RF power dependence of averaged absorption coefficient of AZO thin films.

G. ICP RF power dependence of crystallinity of thin film

Figure 8 shows the change in the X-ray diffraction pattern for ICP RF power of 0, 100, 200, and 300W. The appearance of (002) diffraction peak indicates that the film is good crystalline ZnO, and the peak intensity indicates the degree of crystallization. From Fig.8, we find that the AZO film deposited with planar magnetron discharge without ICP assist had already (002) orientation, and the intensity of (002) peak is increased with increasing ICP RF power. This is because the crystallinity of film is promoted with increasing ICP RF power, since the sputtered particles are more excited and ionized and ion fluxes to the substrate are increased in the ICP, resulting in the elevation of substrate surface temperature.

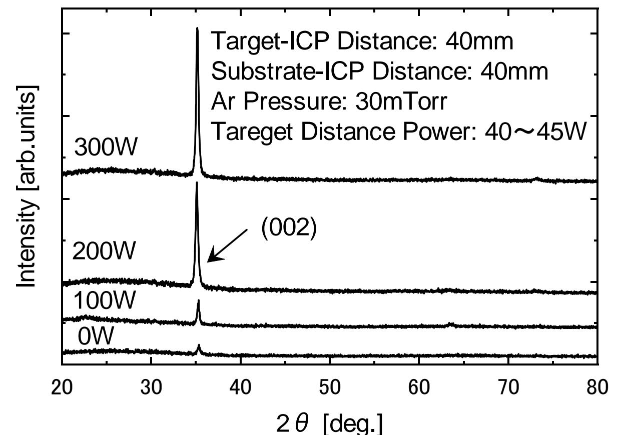

Figure8 ICP-RF power dependence of X-ray diffraction pattern.

H. ICP RF power dependence of elemental ratio in the film

Figure 9 shows ICP RF power dependence of elemental ratio of Al and resistivity in the film. The former was obtained from the XPS analysis of Al 2p signal. With increasing ICP RF power, the elemental ratio of Al in the film increases. Accordingly, the resistivity decreases as shown in Figure 9. The ICP RF power dependence of elemental ratio of Al in the film seems to be in agreement with the dependence of relative

density of Al to Zn atoms in gas phase as shown in Fig.4. The electric conductivity of the AZO film is determined by carrier density and carrier mobility. The former depends on the content of donor Al atoms and the number of oxygen vacancy, while the latter depends on crystallinity of thin films. Thus, it is considered that a rapid decrease in the resistivity is caused not only by the increase in carrier density due to the increase in content of Al atom but also by the increase in carrier mobility due to the promotion of crystallinity of thin film as shown in Figure 8.

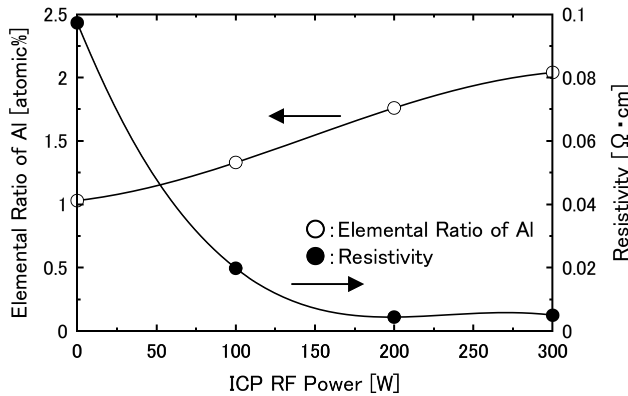

Figure9. ICP RF power dependence of elemental ratio of Al in the film and resistivity.

IV. CONCLUSION

Deposition process of AZO thin films by ICP assisted sputtering was investigated in particular from the view point of influence of ICP RF power. The results obtained in this study can be summarized as follows. All the thin film characteristics (deposition rate, transmittance, resistivity, crystallinity) improve with increasing ICP RF power. Both the relative ratio of Al to Zn atom density in gas phase and the elemental ratio of Al in the deposited film increase with increasing ICP RF power. In addition, crystallinity of AZO film is promoted with increasing ICP RF power. We obtained good quality AZO film with resistivity of $2\times10^{-3}\Omega$cm, transmission of more than 85% at deposition rate of 0.28nm/s at the working pressure of 30mTorr (Ar) with the target power of 40W and with ICP RF power of 300W.

ACKNOWLEDGMENT

The authors wish to thank Dr. Kentaro Sakai of Miyazaki University for his help in XRD and XPS analyses of AZO films. This research was partially supported by a Grant-in-Aid for Scientific Research (C) from the Japan Society for the Promotion of Science (No. 20540485) and by Special Coordination Funds for Promoting Science and Technology sponsored by Japan Science and Technology Agency (JST).

REFERENCES

[1] S. M. Rossnagel and J. Hopwood, "Magnetron Sputter Deposition with high Levels of Metal Ionization," Appl. Phys. Lett., 63 (1993) pp.3285-3287.

[2] J. Hopwood, and F. Qian, "Mechanisms for highly ionized magnetron sputtering," J. Appl. Phys., 78, (1995) pp.758-765.

[3] Y. Matsuda, Y. Koyama, K. Tashiro and H. Fujiyama, "MgO deposition using reactive ionized sputtering," Thin Solid Films, 435 (2003) pp.154-160.

[4] Y. Matsuda, M. Iwaya, Y. Koyama, M. Shinohara, and H. Fujiyama, "Effect of inductively-coupled plasma assist on the crystal orientation of magnesium oxide thin films produced by reactive sputtering," Thin Solid Films, 457, (2004) pp.64-68.

[5] Y. H. Han, S. J. Jung, J. J. Lee, J. H. Joo, "Deposition of MgO films by ICP assisted evaporation," Surf, Coat. Technol. 174-175 (2003) pp.235-239.

[6] S. J. Jung, Y. H. Han, B. M. Koo, J. J. Lee, J. H. Joo," Low temperature deposition of Al-doped zinc oxide films by ICP-assisted reactive DC magnetron sputtering," Thin Solid Films 475 (2005) pp.275-278.

[7] S. Iwai, Y. Matsuda, M. Shinohara, and H. Fujiyama, "Sputter-deposition of aluminum-doped zinc oxide thin films assisted by inductively coupled plasma," Abstracts and full-Paper CD of the 18th Int. Symp. on Plasma Chemistry, August 26-31, 2007, Kyoto, Japan (2007) p.396.

[8] Y. Matsuda, T. Shibasaki, M. Shinohara,"Smoothing of resistivity distributions of sputtered AZO thin film by the assist of ICP," Proc. of the 25th SPP, Yamaguchi, Japan, January 23-25, 2008, A5-01 (2008) pp.79-80.

[9] KONO Akihiro, TAKASJIMA Seigo, HORI Masaru and GOTO Toshio, "Plasma Absorption Spectroscopy Using Microdischarge Light Source," Journal of Nuclear Materials 76 (2000) pp.460-464.

[10] G. V. Samsonov, The Oxide Handbook (IFI/Plenum, New York 1973).